

APPLICATION OF DIGITAL IMAGE CORRELATION TO CAPTURE THE CRACK MOUTH OPENING DISPLACEMENT OF THE NOTCHED STEEL FIBER REINFORCED CONCRETE (SFRC) BEAM

Mudji Irmawan^a, Bambang Piscea^{a*}, Priyo Suprobo^a, Harun Alrasyid^a

Abstract: The application of digital image correlation (DIC) to capture any point in the experimental test is found to be promising. Using the DIC and appropriate tool can overcome the limitation of the traditional sensors to capture the movement or displacement in the tested specimen. In this study, an open-source DIC called Digital Image Correlation Engine (DICE) is used to capture the crack mouth opening displacement (CMOD) of the notched steel fiber reinforced concrete (SFRC) beam with points tracking method. There are three beam specimens with different sizes and similar aspect ratios reported in this paper. All beams have 0.5% steel fiber volumetric content. The SFRC beams are marked with points and tested under a three-point bending flexural test. Custom firmware for Canon DSLR 650D digital camera called Magic Lantern is used to capture the pictures per one second. DICE software is used to analyze the point movements and dumped the output file. ParaView 5.9.0 is then used to visualize the data. A method to calibrate the point coordinate with actual measurement is proposed. A small script is written in Visual Basic Application (VBA) in Microsoft Excel to correlate the displacement for each point of interest with the recorded applied load. With the developed script, any point of interest tracked with DICE can be related to the recorded data from the data logger. From this study, the obtained CMOD with the corresponding applied load is presented, which can be used to investigate the flexural fracture energy of the SFRC beam.

Keywords: Steel fiber reinforced concrete, crack mouth opening displacement, crack propagation, digital image correlation, visual basic

Submitted: 09 August 2022; Revised: 22 December 2022; Accepted: 22 December 2022

INTRODUCTION

The use of digital image correlation (DIC) in the experimental test has now become more popular. It can give more data that can overcome the limitation of the placed sensors in the specimen. The development of DIC has started in the 1970s. In 1985, researcher has detailed the digital image correlation technique formulation used to capture several experiments' rigid-body translation and rotations [1]. From [1], the developed a program and found that the obtained deformation was very accurate, with less than ten percent deformation gradient error. Increasing the image resolution reduces the error in the measurement.

DIC works by analyzing speckled images captured by a solid-state video camera to capture the object state during loading [2]. The changes in the speckled pattern for each captured image are then correlated using an algorithm with a mutual correlation coefficient or other functions to determine the subtle differences. In most cases, a Newton-Raphson method with partial differential correction is still used as the main algorithm to find the subtle displacement [2]. Researchers have also tried to develop a more efficient algorithm to speed up the correlation process.

As outlined above, one can use a solid-state video camera or a still digital image camera to capture the object state during loading. However, the number of frames per second (fps) for each object state is limited. A solid-state video camera can capture sixty fps. On the other hand, a still digital image camera can capture ten fps with custom firmware on the device. With the limitation of data acquisition, it is impossible to capture a high-speed growth of the crack in the specimen (i.e., a plain notched concrete beam). However, DIC can still give accurate and valuable

results for a sample with a mechanism to restrain crack growth. DIC was also found to be very useful to capture localization phenomena [3-5].

This paper presents the application of DIC to capture the crack mouth opening displacement (CMOD) on the notched steel-fiber reinforced concrete beam. The addition of steel fiber into the notched concrete beam can prevent and delay the formation of micro-and macro-cracks [6, 7], which enables the use of DIC to capture the object state when the load-carrying capacity softens. In addition, the use of DIC can overcome the limitation of the clip-gauge instrument, which cannot handle large CMOD.

A digital still image camera Canon DSLR 650D is used to capture the object state during the loading. A custom firmware called Magic Lantern [8] is used to capture the image per one second. The speckled pattern is prepared manually using a marker with the dotted pattern. Three steel-fiber notched concrete beams of different sizes were experimentally tested.

The beam specimen sizes are 700×200×300 mm, 800×200×400 mm, and 1000×200×500 mm, respectively. The volumetric fiber content of the steel fiber is 0.5%. The beams are tested under a three-point bending test. A method to calibrate the point coordinate with measured displacement is proposed. A small script prepared in the Visual Basic for Application (VBA) in Microsoft Excel is also proposed to correlate the high-rate data acquisition and the DIC data.

RESEARCH SIGNIFICANCE

This paper presents the application of DIC to capture the crack mouth opening displacement on the steel fiber notched beam. A custom firmware called Magic Lantern for the Canon DSLR 650D [8] is used to enable an accurate automatic still image capture for every one second. A program called Digital Image Correlation Engine (DICE 2.0, [9]) is used for image correlation purposes. A method

^aLecturer in the Civil Engineering Department, Institut Teknologi Sepuluh Nopember, ITS Campus, Sukolilo, Surabaya 60111, Indonesia. Corresponding author email address: piscesa@ce.its.ac.id

to calibrate with point coordinate with the measured displacement is proposed. A small VBA script is proposed to correlate the high-rate data acquisition device and the DIC data.

METHODOLOGY

Firstly, the research is established by preparing all the necessary experimental work, including specimen preparation and DIC equipment. Besides the practical work, the research also requires studying all the needed software and developing a small script to correlate the data between the high-rate data acquisition device and the DIC data.

A. SPECIMEN MATERIAL AND GEOMETRY DETAILS

The concrete compressive strength for the specimen is design with 30 MPa concrete. The mix design for plain concrete is carried out based on SNI 03-2834-2000 [10] (Department of Environment, DOE method [11]). On the other hand, ACI 544-3R-08 [12] is used to prepare the steel fiber reinforced concrete beam mix design. The type of the steel fiber is Dramix 4D 65/60 BG++ type, which has a diameter of 0.9 mm, length 60 mm, an aspect ratio of 65, Young's modulus of 200 GPa, and yield strength 1600 MPa.

Three notched beam specimens with different sizes were tested. Table 1 showed the geometry details of the specimen. The volumetric fiber content for the steel fiber considered is 0.5%. Figure 1 shows the illustration of the specimen. As shown in Figure 1, each beam has a different notched height which was designed based on JCI-S-002-2003 [13]. The notched width for all beams is set to 5 mm. The height of the beam notched is set to one-third of the beam height.

Table 1 Specimen geometry details

ID	Size (mm) (L×B×D)	Steel Fiber (%)	Quantity (pieces)
B300-1	700 x 200 x 300	0.5	1.0
B400-1	800 x 200 x 400	0.5	1.0
B500-1	1000 x 200 x 500	0.5	1.0

The beam molding is prepared with knock-down steel formwork, which can be used many times. Figure 2 shows the specimen preparation work. In Figure 2a, it is seen that the concrete was cast inside the formwork upside down. The beam notch was positioned at the top of the mold. After 24 hours, the formwork was removed, and the beam is placed in the temporary curing pond made from thick plastic (see Figure 2b). The specimens are water-cured until reaching the age of 28 days. The specimen was removed from the curing pond and remained air dry for several hours before testing.

B. TESTING METHOD AND EQUIPMENT

The testing method is based on a three-point bending test as outlined in ASTM 70. Figure 3 shows the experimental test setup of the beam inside the Universal Testing Machine (UTM). The UTM has 100 tons capacity and is equipped with an analog load cell and stroke measurement device. One load cell with 1.0 MN capacity and one linear variable

displacement transducer (LVDT) is attached at the top loading platen. A digital camera Canon DSLR 650D seated on a tripod is used to capture the digital deformation of the beam by taking the picture every one second. The machine loading control is based on displacement.

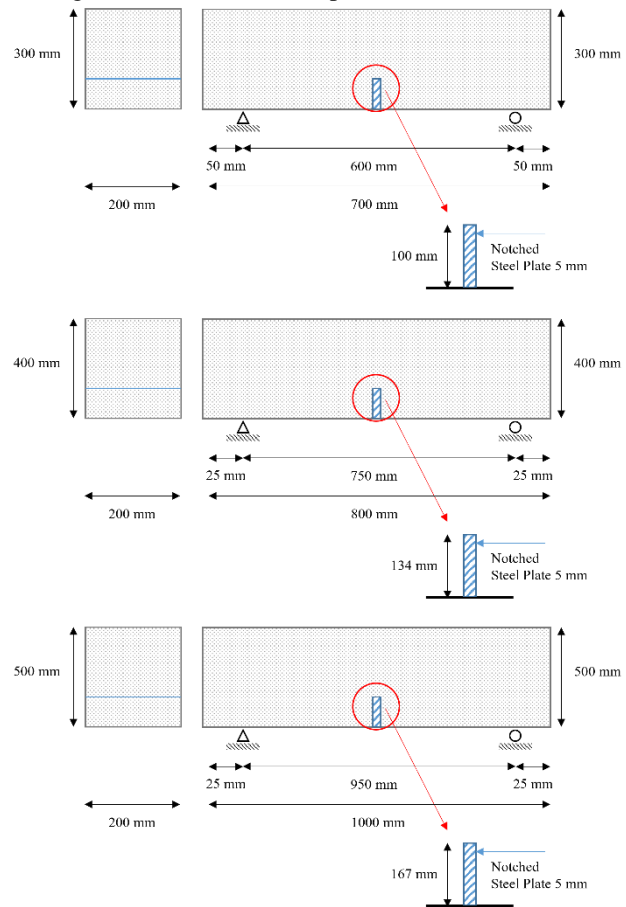


Figure 1 Illustration of the beam geometry detail for each specimen

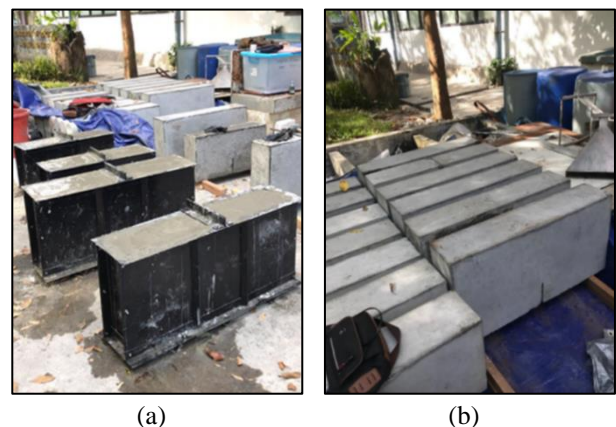


Figure 2 Specimen preparation: (a) during casting inside the mold; (b) after removal of the steel formwork

C. DIGITAL IMAGE CORRELATION

C.1. Preparation (Equipment and DICE Setting)

This research's digital image correlation technique requires a digital still camera to capture a picture per one second. A Canon DSLR 650D digital camera and a custom firmware

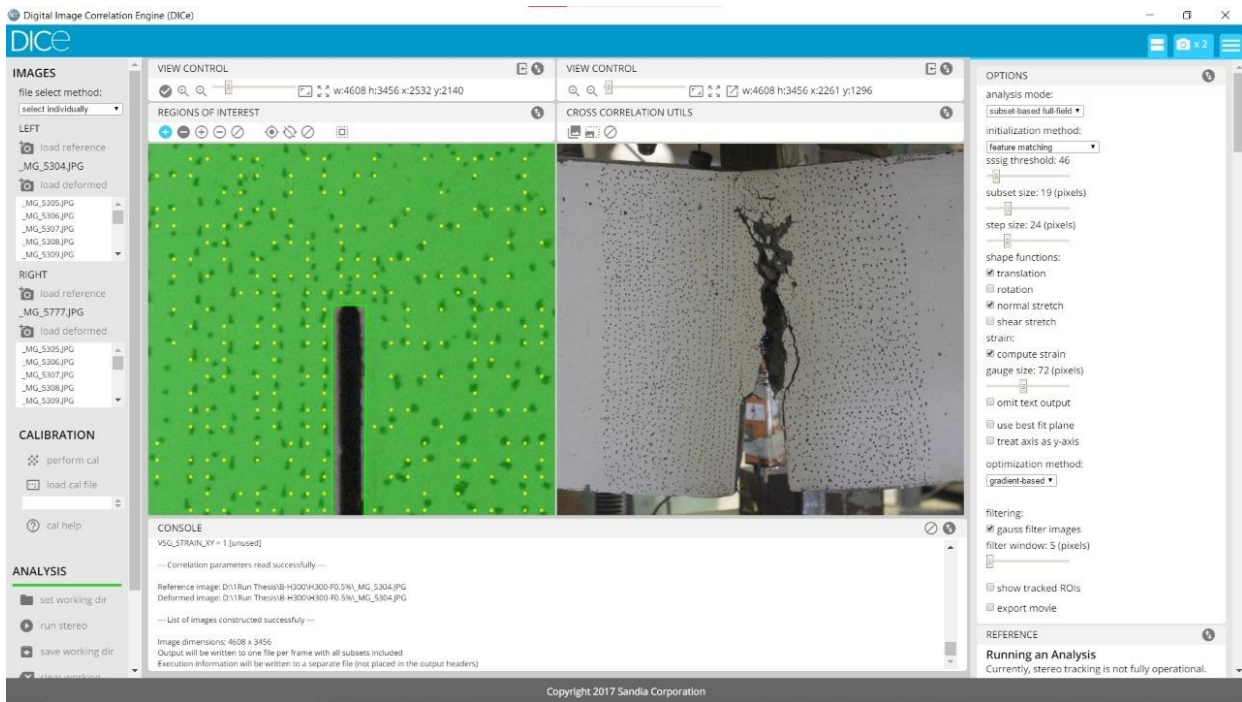


Figure 4 DICE graphical user interface and investigated specimen

called Magic Lantern [8] are used for that purpose. For the software to correlate the deformation of the tested specimen, the specimen must have speckled patterns (random dotted points). In the prepared sample, before testing, one face of the sample was painted white and manually plotted with random dotted points (see Figures 3 and 4).

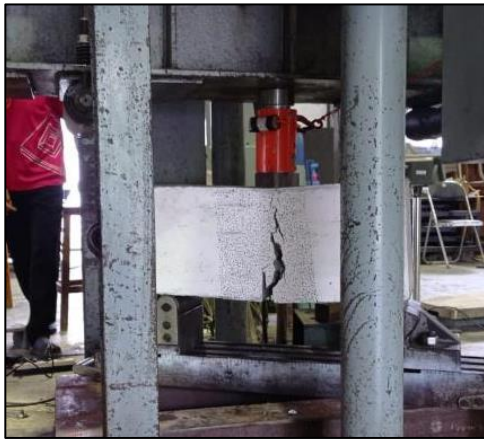


Figure 3 Experimental test set up of the beam inside a 100 Ton UTM

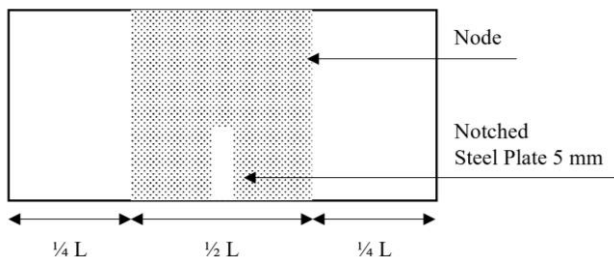


Figure 4 Illustration of random dotted points in the notched beam specimen

Once the test is completed, the saved picture is processed using a DIC software called Digital Image Correlation

Engine (DICE, [9]). DICE is a copyrighted open-source DIC tool that is stand-alone and easy to use [9]. The full-field displacements and strains can be obtained by analyzing digital images containing the speckled patterns and tracking objects' rigid body motions. DICE also provides an extended data output to be viewed using ParaView 5.9.0 software [14, 15] which is very useful for calibration purposes and extracting specific data as a function of time at any point.

Figure 4 shows the DICE [9] graphical user interface and the notched beam example being analyzed. In Figure 4, the green area is the region of interest and is consisted of the black dotted speckled pattern. In addition to the black dotted speckled pattern, which was shown to be behind the green layer, a yellow dotted pattern coincides with the black dotted speckled pattern. This yellow dotted speckled pattern was generated with a specific option in DICE. The analysis mode is set to subset-based full field. The initialization method is feature matching with SSSIG threshold equal to 46, subset size equal to 19 pixels, and step size equal to 24 pixels. The option of translation and normal stretch in the shape functions are enabled. The strain is computed with a gauge size equivalent to 72 pixels. The gradient-based method is used for optimization, and filtering is based on gauss filter images with a filter window set to five pixels.

C.2. Calibration (Scaling Parameter)

The extracted output data from the DICE 2.0 [9] to ParaView 5.9.0 are based on the pixel resolution and did not reflect the actual measurement in length. Therefore, a calibration is required to further correlate the size from the image to the actual measured distance. In this paper, a simple scaling calibration is proposed. Since the height of the beam is known, say for the beam with size $600 \times 200 \times 300$, the height (h_{beam}) is 300 mm, it is possible to compute the scaling parameter as:

```

Option Explicit
Dim i As Integer, j As Integer

Sub interpolate()
Dim nump As Integer
Dim numcmmod As Integer
nump = Sheet3.Cells(1, 9)
numcmmod = Sheet3.Cells(2, 9)
Dim delta(100000) As Double
Dim p(100000) As Double
Dim cmode(1000) As Double
Dim deltaneu(1000) As Double
Dim pnew(1000) As Double

' Load Data P (from load cell) vs Delta (at the loading platen from LVDT)
For i = 1 To nump
    delta(i) = Sheet3.Cells(i + 1, 1)
    p(i) = Sheet3.Cells(i + 1, 2)
Next i
' Load Data CMOD (from DICE) vs Delta (at the loading platen from DICE)
For i = 1 To numcmmod
    cmode(i) = Sheet3.Cells(i + 1, 5)
    deltaneu(i) = Sheet3.Cells(i + 1, 6)
Next i

' Do Interpolation
For i = 1 To numcmmod
    For j = 2 To nump - 1
        If (deltaneu(i) < delta(j)) Then
            pnew(i) = (deltaneu(i) - delta(j)) / (delta(j) - delta(j - 1)) * (p(j) - p(j - 1))
                + p(j - 1)
            Sheet3.Cells(i + 1, 7) = pnew(i) ' APPLIED LOAD AS FUNCTION OF CMOD
            GoTo 1
        Else
            If j = nump - 1 Then
                pnew(i) = 0
                Sheet3.Cells(i + 1, 7) = pnew(i) ' APPLIED LOAD AS FUNCTION OF CMOD
                GoTo 1
            End If
        End If
    Next j
1:
Next i
End Sub

```

Figure 5 Developed VBA code to correlate the applied load with CMOD

$$\chi = \frac{h_2 - h_1}{h_{beam}} \quad (1)$$

Where h_2 and h_1 are the top and bottom points coordinate obtained from the ParaView, representing the beam's height from the image. Once the scaling parameter (χ) is obtained, any extracted data points from ParaView which may represent the displacements and strains must be scaled with the scaling parameter to get the actual displacements or strains.

C.3. Correlation (P-CMOD)

A bridging variable that shares the exact measurement must correlate between the applied load (P) and the crack mouth opening displacement (CMOD). The recorded data were the applied load (P) and the vertical displacement at the mid-span measured by the LVDT (Δ_{mid}) from the data logger. On the other hand, from DICE and ParaView, the obtained data were the crack mouth opening displacement (CMOD) and the vertical displacement at the mid-span (Δ_{mid}). Therefore, to relate P with CMOD, Δ_{mid} can be used as the bridging variable. However, the time step between the vertical displacement at mid-span from LVDT and DICE is not similar. Therefore, a small VBA code is

developed with a linear interpolation method to directly relate the applied load (P) with the CMOD.

Figure 5 shows the developed code in VBA to connect the CMOD with the applied load. The code works by equating the mid-span displacement from the LVDT with the mid-span displacement from the DICE. Since the displacement from LVDT relates to the applied load from the load cell, and the displacement from the DICE relates to the CMOD from DICE, it is possible to have the applied load (P) plotted as a function of the CMOD.

ANALYSIS RESULTS AND DISCUSSIONS

A. LOAD-DISPLACEMENT RELATIONSHIP

Figure 6 shows the load-displacement curve for all the tested specimens. In Figure 6, the x and y axes define the applied load (P) and the mid-span displacement (Δ_{mid}), respectively. As shown in Figure 6, as the specimen size increases, the peak load carrying capacity also increases, implying that the size effect exists for steel fiber reinforced concrete. The peak loads for B300-1, B400-1, and B500-1 are 51.09 kN, 57.64 kN, and 60.36 kN. The softening response of the load-displacement curve was almost similar. At the mid-span displacement of approximately 15 mm, the residual load for B400-1 was only slightly higher

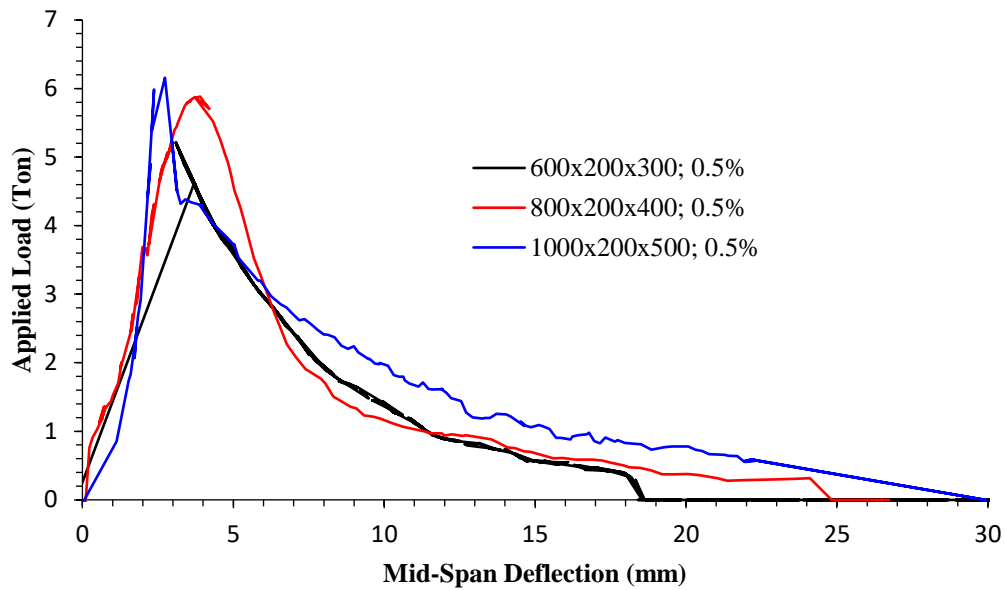


Figure 6 RC deep beam forces and design stress ratio with the second objective function

than B300-1 which showed that the residual load level for both specimens was almost similar. The specimen's mid-span displacement at zero load-carrying capacity for B300-1, B400-1, and B500-1 are 18.86, 24.82, and 29.91 mm, respectively.

B. DICE AND PARAVIEW OUTPUT

The output data from the DICE software is opened using ParaView 5.9.0. Figure 7 shows the dotted pattern nodes in the notched area (undeformed state). As shown in Figure 7, all the nodes had blue color, meaning zero displacements.

Figure 8 shows the dotted pattern nodes in the notches area. Notice that the color of the left-hand side nodes differs from the right-hand side nodes. Both nodes in each direction also move away from the notches, which clearly show the notch opening. In Figure 8, some dark blue nodes existed that may not have significant movement due to the yellow dotted speckled pattern in each captured picture was not present. It is also possible that DICE was not successful in tracking all the node's movements. These non-displaced node movements can be ignored and obtaining the required movement at the notch edges can be done by selecting the appropriate node that is tracked for every step.

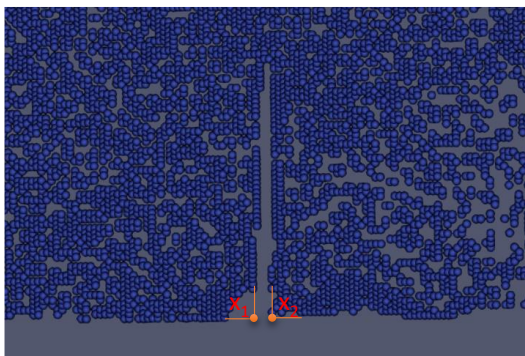


Figure 5 Dotted pattern nodes in the notched area (undeformed state)

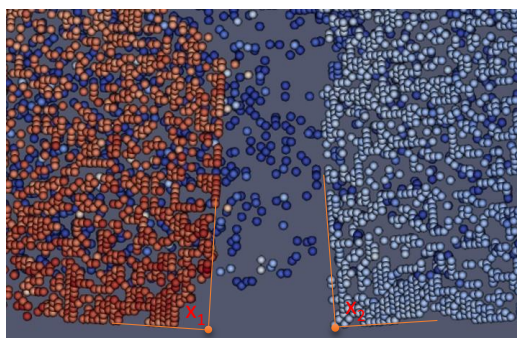


Figure 6 Dotted pattern nodes in the notched area (deformed state)

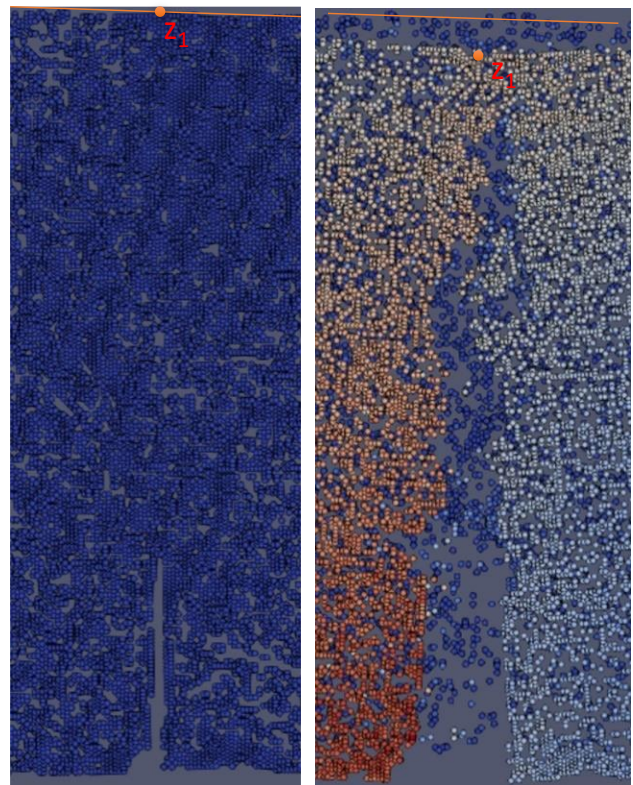


Figure 7 Reference point deflection on center span, early step (left), last step (right)

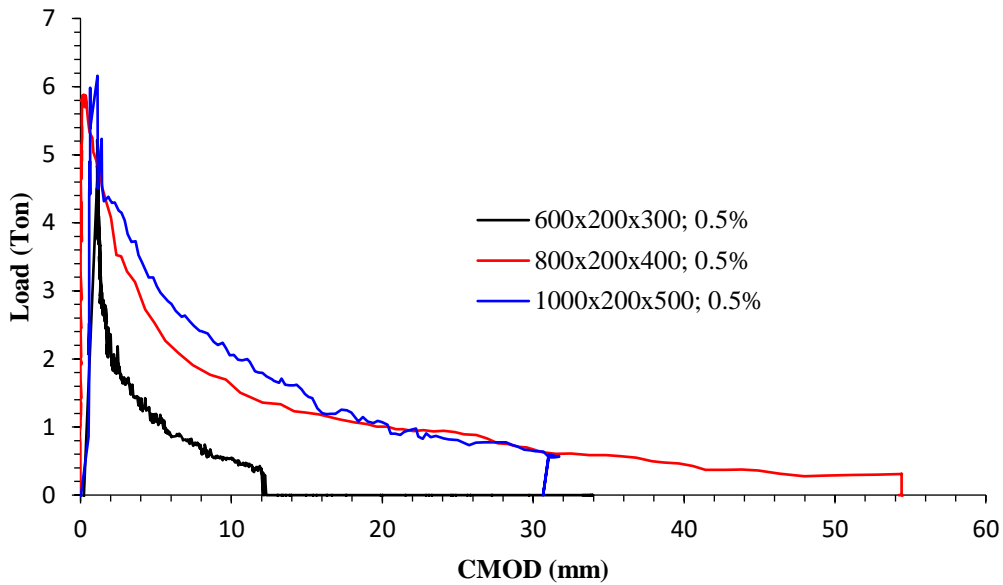


Figure 10 RC deep beam forces and design stress ratio with the second objective function

In Figure 7, there are two yellow dots where the left one is noted as x_1 and x_2 . For x_2 it is easy to pick the closest available node. However, for x_1 since there is no existing node at the edge of the notch, the value for x_1 can be approximated using a simple extrapolation technique from two nodes at the left-hand side wall of the notch. The CMOD at every time step can be easily obtained by subtracting the horizontal displacement at point x_2 (positive, moving to the right) with the horizontal displacement at point x_1 (negative, moving to the left). In Figure 8, the movement of points x_1 and x_2 contributed to the CMOD. Hence, to correlate the CMOD with the recorded applied load from the load cell, the data of the mid-span displacement from DICE should also be extracted using the same method as extracting the CMOD from the DICE output data.

Figure 9 shows the region of interest (ROI) (from bottom to top of the beam) at the undeformed state (left) and displaced state (right). In Figure 9, the crack pattern was seen clearly. Figure 9 also shows that at the loading platen in the mid-span, the point at that location also displaced in the vertical direction (see orange-colored node with z_j notation). The node's movement in loading platen is noted as the mid-span displacement from DICE (Δ_{mid}). Hence, from DICE and ParaView, the corresponding mid-span displacement (Δ_{mid}) and the crack mouth opening displacement (CMOD) can be obtained.

C. LOAD-CMOD RELATIONSHIP

The load-CMOD relationship can be obtained by executing the developed VBA code in Figure 5. The input required in the VBA code is the applied load from the load cell (P), the mid-span displacement from the LVDT (Δ_{mid}), the mid-span displacement from the DICE and ParaView (Δ_{mid}), and the crack-mouth opening displacement (CMOD) from the DICE and ParaView. The output from the VBA code is the applied load (P) and the crack-mouth opening displacement (CMOD).

Figure 10 shows the load-CMOD relationship for the tested specimen. The area beneath the load-CMOD relationship can be related to the fracture energy of the beam due to flexure. From Figure 10, it is seen that as the size of the specimen increases, the area beneath the load-CMOD curve increases. The size of the area beneath the load-CMOD curve showed that the size of the specimen affects the flexural fracture energy. However, further investigation should be carried out to back-calculate the uniaxial tensile fracture energy for SFRC. It may be possible that the uniaxial tensile fracture energy of SFRC is size-independent.

Unlike the load-displacement curve, there is no softening curve crossing for B300-1 and B400-1 in the load-CMOD curve. In contrast, the load-CMOD curve for B400-1 when softens only slightly lower than B500-1. In addition, the final CMOD for B400-1 was found to be the longest compared to B500-1 and B300-1. The final CMOD for B300-1, B400-1, and B500-1 are 12.84, 31.39, and 54.44 mm.

CONCLUSIONS

This paper has presented an application of digital image correlation to capture the crack-mouth opening displacement (CMOD) of the notched steel fiber reinforced concrete (SFRC) beam. A digital camera DSLR Canon 650d with Magic Lantern [8] custom firmware was used to capture the picture of the sample for each second. The authors used an open-source Digital Image Correlation Engine (DICE) software to process the captured picture and dump the output to be viewed using ParaView 5.9.0. Detailed discussion on extracting the displacement data (CMOD and Δ_{mid}) in ParaView 5.9.0 was presented.

A simple method to calibrate the software measurement with the actual measurement was proposed. The scaling method was proposed by simply comparing two points in the extracted node in ParaView 5.9.0 with the exact height of the beam. The author developed a small VBA code to correlate the applied load (P) and the crack-

mouth opening displacement (CMOD). It was made possible to get the flexural fracture energy for each specimen using the proposed procedure to correlate the applied load (P) with the crack-mouth opening displacement (CMOD).

From the load-displacement curve of the tested specimen, it was found out that the peak load of the notched SFRC beam was affected by the size of the sample. The load-CMOD curve result also found out that the size of the specimen affected the flexural fracture energy. However, further analysis to back-calculate the uniaxial tensile fracture energy using inverse analysis should be carried out. The back-calculated load-crack opening displacement curve can be used for non-linear finite element simulation.

REFERENCES

- [1] T. C. Chu, W. F. Ranson, and M. A. Sutton, "Applications of digital-image-correlation techniques to experimental mechanics," *Experimental Mechanics*, vol. 25, no. 3, pp. 232-244, 1985.
- [2] P. C. Hung, and A. S. Voloshin, "In-plane strain measurement by digital image correlation," *Journal of the Brazilian Society of Mechanical Sciences and Engineering*, vol. 25, no. 3, pp. 215-221, 2003.
- [3] J. N. Périé, S. Calloch, C. Cluzel, and F. Hild, "Analysis of a multiaxial test on a C/C composite by using digital image correlation and a damage model," *Experimental Mechanics*, vol. 42, no. 3, pp. 318-328, 2002.
- [4] B. Wattrisse, A. Chrysochoos, J. -M. Muracciole, and M. N. Gaillard, "Analysis of strain localization during tensile tests by digital image correlation," *Experimental Mechanics*, vol. 41, no. 1, pp. 29-39, 2001.
- [5] Y. Berthaud, S. Calloch, C. Cluzel, F. Hild, and J. N. Périé, "Experiment/computation interactions by using digital image correlation," in *Interferometry in Speckle Light*, 2000, Springer, pp. 59-66.
- [6] D. -L. Nguyen, M. N. -T. Lam, D. -J. Kim, and J. Song, "Direct tensile self-sensing and fracture energy of steel-fiber-reinforced concretes," *Composites Part B: Engineering*, vol. 183, p. 107714.
- [7] M. Maksum, H. Alrasyid, M. Irmawan, and B. Piscesa, "Effect of steel fiber volume fraction to the tensile splitting strength of concrete cylinder" in *IOP Conference Series: Materials Science and Engineering*. 2020, vol. 930, IOP Publishing, p. 012058
- [8] T. Hudson, Magic lantern for 650D / rebel T4i. Magic Lantern Development Team, 2018.
- [9] D. Turner, Digital Image Correlation engine (DICE) reference manual, sandia report, SAND2015-10606 O. Copyright 2015 National Technology & Engineering Solutions of Sandia, LLC (NTESS), 2015.
- [10] B. S. Nasional, Tata cara pembuatan rencana campuran beton normal (SNI 03:2834-2000). (Jakarta:Standar Nasional Indonesia). 2000
- [11] D. C. Teychenné, H. C. Erntroy, R. E. Franklin, Design of normal concrete mixes. HM Stationery Office, 1975.
- [12] A. C. I. 544, Guide for specifying, proportioning, and production of fiber-reinforced concrete. American Concrete Institute, 2008.
- [13] J. C. I. S-002-2003. Method of test for load-displacement curve of fiber reinforced concrete by use of notched beam. Japan Concrete Institute Standard, 2003.
- [14] J. Ahrens, B. Geveci, and C. Law, ParaView: An End-User Tool for Large-Data Visualization. The Visualization Handbook, 2005.
- [15] U. Ayachit, The paraview guide: a parallel visualization application. Kitware, Inc., 2015.